Special Issue

Accelerated Testing and Failure of Thin-film PV Modules

T. J. McMahon[*,†]

National Renewable Energy Laboratory, 1617 Cole Boulevard, Golden, CO 80401, USA

Packaging-related PV module failure is distinguished from cell failure, and those failures specific to thin-film modules are reviewed. These are categorized according to the type of stress that produced them, e.g., temperature, voltage, moisture, current, and thermal cycling. An example is given that shows how to relate time under accelerated stress to time in use. Diagnostic tools for locating the affected area within a large-area module are pointed out along with the importance of interpretation of the visual appearance of the different damage mechanisms. Copyright © 2004 John Wiley & Sons, Ltd.

INTRODUCTION

The U.S. Department of Energy encourages and supports the photovoltaic (PV) industry in developing a module technology that will last 30 years in the field.[1] An additional goal is to identify a short-term means to certify that a module technology will, indeed, last 30 years. The achievement of the first goal for thin-film (TF) PV modules will be more difficult than for the single- and multi-crystalline Si modules that have been available for some time. There are at least four reasons for this: (1) TF cells have a lower threshold for corrosion and delamination; (2) several of the amorphous Si and CdTe TF technologies use the SnO_2-coated soda-lime glass superstrate configuration requiring an edge-deleted module perimeter; (3) SnO_2-coated glass under high cell-to-frame voltage conditions and humidity can cause delamination of the SnO_2/glass interface; and (4) TF module configurations usually lack the extra isolation that is afforded by extra layers of laminating material (EVA or thermoplastic) found in non-TF modules.

Regarding the second goal, arguments have been made that achievement of a test protocol to certify a 30-year lifetime is not possible.[2] Short of such a 30-year lifetime certification process, an approach for rank ordering and testing of failure modes has been developed; R. G. Ross[3] has put forth another method that rank orders mechanisms according to analysis of the 'life-cycle energy cost impact'. Rank ordering allows the PV industry to address the more pressing problems first, without the encumbrance of complicated lifetime-prediction methdologies. Recently, M. A. Quintana *et al.* have reported commonly observed degradation in field-aged PV modules.[4]

The visual appearance of many failure mechanisms related to packaging can be very striking. Any one of the TF layers can be damaged from corrosion, electrolytic electromigration, diffusion, cracking, and delamination. Especially notable are the effects of glass corrosion. Each of the failure mechanisms that results in visual

damage has its own appearance. Considerable progress can be made in understanding module-packaging failure if proper interpretation of the visual damage is provied by an astute observer. The following is a review of failure mechanisms and strategies special to the certification and analysis of TF module reliability. Much of this work was carried out at the Jet Propulsion Laboratory (JPL) in the 1980s under the direction of R. Ross; these references are vital as this review is not a stand-alone publication.

FAILURE

Before proceeding, we must define terms such as 'failure'. As a starting point we paraphrase a textbook definition[5] of 'reliability' as it might apply to our case: 'a reliable PV module has a ''high probability'' that it will perform its intended purpose adequately for 30 years, under the operating conditions encountered'. For simplicity, and by way of example, we could say a PV module fails to provide service if its power output decreases by more than 30% before 30 years, i.e., 1%/yr, in its use environment. Also, 'a high probability' could mean that 95% of the modules in the field will achieve this success. By 'use environment', we mean any and all use environments that the PV module will experience during service. Site meteorology, handling, and installation are included in use-environment considerations.

It is useful to divide the failures that occur in TF modules into two categories: (1) cell-related; and (2) packaging-related. *Cell-related* failures are caused by use-environment stress, such as temperature, that packaging cannot protect against. Also, because no packaging can be perfect, TF cells must tolerate low levels of pollutant gases or water vapor. These levels will depend on the TF Technology and related device processing. Cell-related failure mechanisms will not be a topic of this paper, except when they are directly related to packaging failure.

Packaging-related failures occur when pollutant gas (admitted from the outside or generated from within) or water vapor levels are elevated at the cell, cell interconnect, or bus-line interconnects to levels that induce damage that diminish module output power at a rate of more than 1%/yr. They may also cause loss of electrical isolation of cells from ground, loss of structural integrity, or visual defects that are unsatisfactory to the user. Other kinds of packaging failures occur when incompatible materials are used; because of thermal expansion mismatch, creep, loss of adhesion, galvanic corrosion, etc., module packaging may be compromised.

DIAGNOSTICS FOR LOCATING FAILURE

Depending upon the detailed nature of the failure, different aspects of the *I–V* curve will be impacted, so it is essential to carry out rigorous characterization in the dark and light. It can be difficult to identify the bad cell(s), let alone bad areas within a cell, because of the complication of having to deal with the encapsulated series-connected package. In such a module, the individual cell cannot be de-encapsulated without further damaging the electrical performance of an already damaged or undamaged TF cell. Simple circuit-simulation programs such as Pspice can simulate the effect of a single cell or several cells on the module *I–V* characteristic, such as 'kinks' or inflection points in a light or dark *I–V* curve for the two-terminal series-connected output. Thus the effects of a supposed cell damage can be ruled in as a possibility or ruled out. While Pspice simulates the behavior of series and parallel combinations of ideal solar cells, the *I–V* curves of TF solar cells can be best studied by electronic device simulation software such as AMPS.[6] The non-ideal behavior of CdTe cells is an example of this kind of device simulation.[7]

Fairly innovative diagnostics can identify which cells are not performing. A heat-sensing technique such as a thermochromic paper, infrared camera, or a light-spot scanning technique, can precisely locate affected areas. Figure 1 shows an example of an infrared image of the front of a TF module, which is covered with 3-mm-thick soda-lime glass, in forward bias to reveal series resistance or current flow problems. Reverse-bias images can be used in a similar manner to reveal and locate shunting problems because higher current density, hence thermal dissipation, is experienced. The best images for glass-laminated modules in terms of brightness and contrast can be obtained after a 2-min period of current bias.[8]
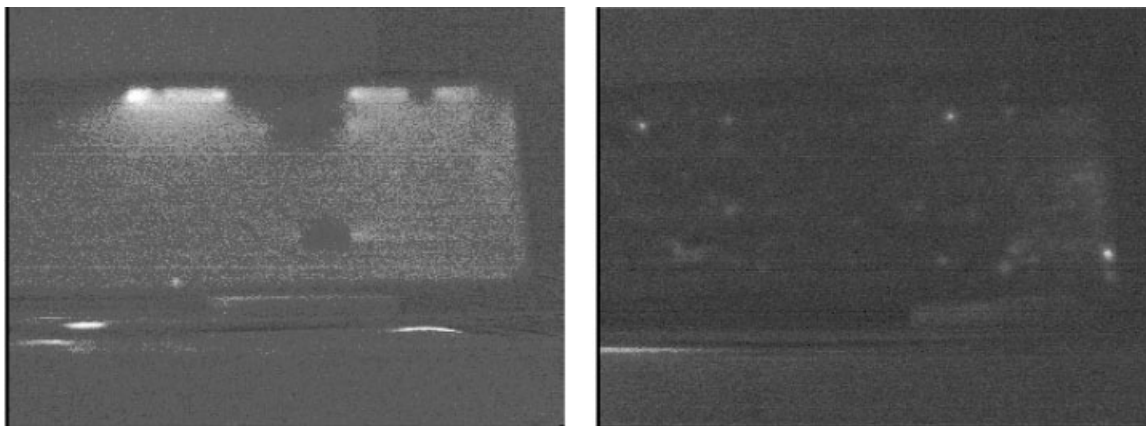
Figure 1. Infrared images of the same TF module in forward (left) and reverse bias (right)

Additionally, non-destructive individual cell shunt resistance values can be determined on a cell-by-cell basis. Two methods that avoid the need of opening up a module, a process that would very likely cause further damage to the TF cells, have been developed. An electrical modulation technique developed at NREL involves selectively shading the cell of interest and leaving the rest in constant light. An a.c. current is measured across the two terminals of the module as the result of a small applied oscillating voltage about V_{oc} to obtain the dark resistance of the darkened cell.[9] A d.c. electrical technique[10] involves illuminating the cell in question and determining its V_{oc} and I_{sc}. Clever photomodulation techniques are also available to examine the cell in question.[11–13]

ACCELERATED ENVIRONMENTAL TESTING

Accelerated environmental tests (AETs) can be used in a number of ways such as a standardized screening test. Screening tests require a small number of test samples to accelerate and isolate failure modes and can be performed on mini-modules or cell structures as well as on full-sized modules. The basic approach is to prioritize failure modes to be investigated, design and perform AETs to fully characterize each individual failure mode (in terms of relevant environmental stresses), and repeat the process with each succeeding failure mode until all are understood. In this way, these screening tests will reveal relevant failure mechanisms and allow acceleration factors to be determined for the different models that are used in a second type of AET, namely, life-prediction tests. Care must be taken to test for failure mechanisms that will occur in the field and not to accelerate ones that will not.[14] This protocol is used to identify inferior processes, materials, or designs.

Lifetime-prediction tests appropriate for full-sized modules are possible only when a final module design is defined, all failure modes are identified for that module design, and acceleration parameters for each relevant environmental stress are known. The AETs chosen must use stress or combinations of stresses that will accelerate failure modes that actually occur in the use environment. Module lifetime in Colorado may be very different from that in Florida or Bahrain. We must decide which performance parameter(s) should be measured to best monitor the failure mode being evaluated and then define what constitutes a failure for that performance parameter. Traditionally, only module power output is monitored. Some failures might be best studied with another more sensitive parameter as described below. Acceleration parameters must be determined through correlation of damage caused by accelerated laboratory stress to damage occurring outside in the field. Careful monitoring of relevant meteorological parameters in the field must be carried out at all sites.

To use AETs for life-prediction testing, it is best to divide the protocol into five steps: (1) identify and isolate all failure modes, e.g., in a c-Si module we might look at solder-bond fatigue or in a TF module it might be film adhesion or moisture intrusion; (2) design and perform AETs, e.g., thermal cycling with series resistance as a metric or damp heat with visual area of damage as a metric; (3) use appropriate statistical distributions to model

specific failure rates; (4) choose and apply relevant acceleration models to transform failure rates; (5) develop a total module failure rate as a composite of individual rates to allow service-lifetime prediction for each use condition.[15] It is important to understand the dominant mechanisms underlying degradation to allow transformation from life at accelerated stress to life at use-stress conditions, and to allow problems to be remedied and improvements in reliability to be made.

Few examples exist in which a PV product was stressed in an indoor chamber and had the degraded results correlated with outdoor tests. One study looked at diminishing short-circuit current in crystalline Si modules where UV dose was the metric of consequence.[16] These tests were not very accelerated; the highest factor was in the 3X outdoor system. There is much more extensive work on correlation and life prediction in the paint and coatings industry. Even with these presumably simpler systems, usually involving polymers, correlation is often lacking.[17] A report on 50-100X UV accelerated degradation of bilayer coatings shows good success at predicting performance change for outdoor sites in Golden, CO and Phoenix, AZ. The failure model uses the effects of UV dose and temperature.[18] I know of no documentation on accelerated aging of TF PV products where correlation to outdoor sites such as these were made.

In fact, development of a test protocol composed of a series of AETs to derive a service-life prediction applicable to *some arbitrary TF module* is not possible.[2] AETs are more generally used as a screening tool for module design and materials. Two standard screening test protocols in the United States are UL 1703 for safety[19] and IEEE 1262 PV module qualification testing for minimum standards.[20] Europe has developed the IEC1215 qualification tests as its own standard.[21] The IEEE 1262 test sequence was developed by committee procedures and, for the most part, based on JPL block V standards developed for the Si module industry[22] in 1981. Though some correlation to field test results in Miami, FL were established, a rigorous methodology was not used to develop these standards. Modifications were made to accommodate the TF technologies; a special annealing cycle for a-Si was added and an equilibrium light exposure for CIS is being considered. For the most part, however, these standards remain and their relevancy is based on results for Si modules in the field. Assurance that these tests are valid for TF modules, or for that matter, Si modules, has not been established. The so-called 'damp heat test' or '85°C/85 RH for 1000 h' is a difficult sequence to pass, especially for TF modules. It has, however, served as a good screening tool for Si modules.

A number of known and suspected failure modes are listed in Table I, along with possible failure mechanisms that could lead to these failure modes. The cell failure modes are separated from the module modes. In the case of CIGS modules, J. Wennerberg *et al.* have quantified the effect of humidity on the sheet resistance of the ZnO and subsequently on the cell's degradation and the overall module degradation. To explain *all* the module performance loss, the authors invoke scribe-line interconnect resistance increases caused by oxide formation and/or free-carrier depletion at the ZnO:Al/Mo contact interface.[23]

The key to the application of accelerated testing for screening and life-prediction purposes[30] is the relation of time at use stress t_u to time at elevated/accelerated stress t_s via a linear acceleration factor a_i:

$$t_u = a_i t_S, \tag{1}$$

where the failure mechanism for accelerated conditions is assured to be the same as that experienced during field conditions. The type of failure mechanism involved can be used to develop a functional expression for a_i in terms of relevant stress parameters. It is important to do the correlation work to have an idea of how high the accelerated stress levels are or if, in fact, any accelerated stress level is being applied. Testing and failure due to the following five acceleration stresses (temperature, voltage, moisture, current, and thermal cycling) are discussed in turn.

Temperature

Diffusion of contaminates, metals, or dopants and oxide formation are examples of thermally driven failure mechanisms that are usually related to cell failure. Diffusion of Al into a-Si can initiate crystallization processes as well as increase resistance of the Al contact.[29] Surface or bulk electrical conductivity, such as for soda-lime glass, can cause module failure. An Arrhenius treatment may be appropriate for each of these.

Table I. Thin-film failure modes and failure mechanisms

Failure modes	Effect on *I–V* curve	Possible failure mechanisms
1. Cell degradation		
a. Main junction: increased recombination[24]	Loss in fill factor, I_{sc}, and V_{oc}	Diffusion of dopants, impurities, etc. Electromigration
b. Back barrier; loss of ohmic contact (CdTe)[7,24,25]	Roll-over, cross-over of dark and light *I–V*, higher R_{ser}	Diffusion of dopants, impurities, etc. Corrosion, oxidation Electromigration
c. Shunting[26–28]	R_{shunt} decreases	Diffusion of metals, impurities, etc.
d. Series; ZnO,[23] Al[29]	R_{ser} increases	Corrosion, diffusion
e. De-adhesion SnO_2 from soda-lime glass[57,59]	I_{sc} decreases and R_{ser} increases	Na ion migration to SnO_2/glass interface
f. De-adhesion of back metal contact	I_{sc} decreases	Lamination stresses
2. Module degradation		
Interconnect degradation		
a. Interconnect resistance; ZnO:Al/Mo or Mo[23], Al interconnect[49]	R_{ser} increases	Corrosion, electromigration
b. Shunting; Mo across isolation scribe[23]	R_{shunt} decreases	Corrosion, electromigration
Busbar degradation	R_{ser} increases or open curcuit	Corrosion, electromigration
Solder joint	R_{ser} increases or open circuit	Fatigue, coarsening (alloy segragation)
Encapsulation failure		
a. Delamination[36–38]	Loss in fill-factor, I_{sc}, and possible open circuit	Surface contamination, UV degradation, hydrolysis of silane/glass bond, warped glass, 'dinged' glass edges, thermal expansion mismatch
b. Loss of hermetic seal		
c. Glass breakage		
d. Loss of high-potential isolation[50,56,57]		

Since *T* is the simplest stress parameter to deal with, I will use it to illustrate the general principles noted above and provide a method to relate time at *T* in an AET to time at several use sites. In such a case, the form of the acceleration function[30] can be used to relate the time-dependent loss in performance (degradation) $\Delta P(t)$ at a particular elevated temperature T_S as:

$$\Delta P(t) = A e^{-E/T_S} \Delta t. \tag{2}$$

The life at this stressed condition, t_s is the time, Δt at which performance degrades below some level that defines failure. $P(t)$ is measured at intervals of AET exposure to an elevated, laboratory-controlled temperature T_s. The activation energy E is obtained by fitting the data to Equation (2) for at least three values of T_s, with one near or at T_u. Once E is known, the Arrhenius acceleration factor can be used in Equation (1) to obtain time to failure (lifetime) at a given use temperature T_u as:

$$t_u = t_s \exp\left\{ -E\left[\frac{1}{T_s} - \frac{1}{T_u} \right] \right\} \tag{3}$$

Of course, in real-world operation, a single, constant use-temperature is not realistic. To project field life at a specific location characterized by the yearly temperature distribution shown in Figure 2, the time, t_{uj} at each use-temperature experienced T_{uj}, is used to establish the relationship for the lifetime at this site t_u to the time t_s that the module must be held at a constant T_s:

$$t_u = \frac{1}{\sum_j \dfrac{\gamma_j}{t_{uj}}} = \frac{t_s}{\sum_j \gamma_j \exp\left\{ E\left[\frac{1}{T_s} - \frac{1}{T_{uj}} \right] \right\}} \tag{4}$$

where γ_j is the number of hours per year that the module experiences T_{uj} divided by the number of hours in a year. The results of Equation (4) are plotted in Figure 3 where the time at a constant stress temperature required
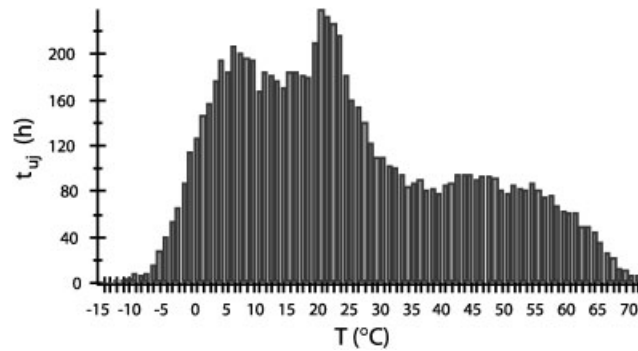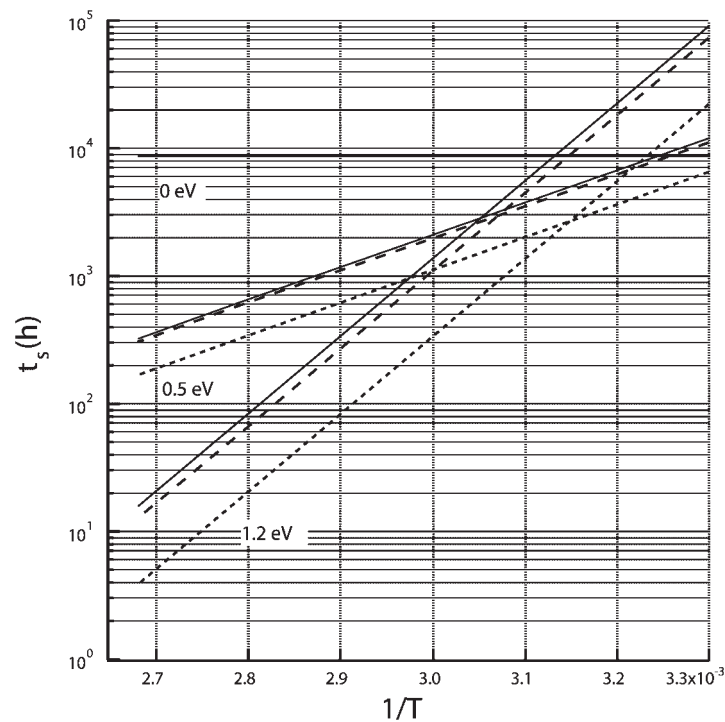
Figure 2. Back-of-module temperatures for Las Cruces, NM

Figure 3. Stress time, t_s to simulate 1 year at Superior, CA (solid lines), Las Cruces, NM (dashed lines), and Golden, CO (dotted lines), for $E = 0$, 0·5, and 1·2 eV[15]

to simulate 1 year of exposure at three different sites is shown for three activation energies. Note that for $E = 0$ eV, there is no temperature dependence and all three sites degenerate into one horizontal line at $t_s = 8670$ h. The results shown in this graph are quite general and, in a concise way, define how much stress time t_s is required at a specific T for each of three E values to simulate 1 year at each of the three sites for a thermally activated process.

Temperature can accelerate adhesive and cohesive failure in double-glass-laminated modules due to residual strain in the glass after lamination. Bubbles, as shown in Figure 4 are caused when a double-glass-laminated module has a front or back cover glass that is not flat, resulting in a large amount of strain after the lamination process. In an a-Si module, adhesive and cohesive failure occurs between the EVA and back metallization. In CdTe modules, de-adhesion is a mixture of back metallization pulling off the cell and EVA delaminating from the back metal. Figure 4 also shows how EVA forms viscous fingers[31] as a bubble forms between the EVA and
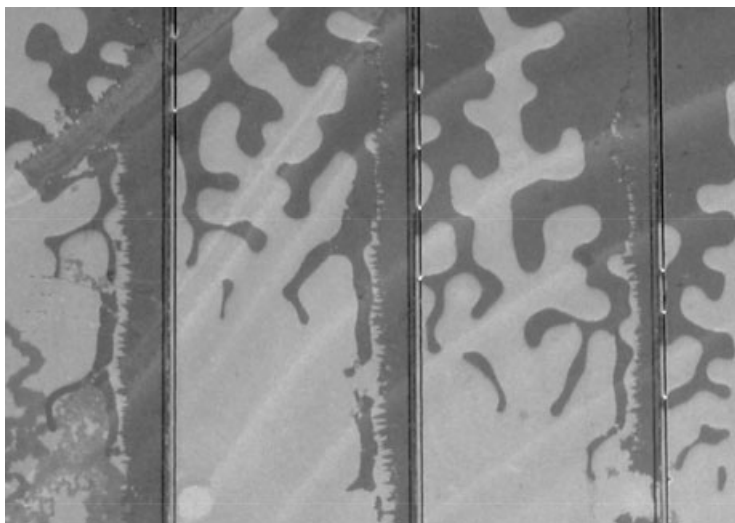
Figure 4. Back cover-glass view at the edge of a delamination bubble due to warped glass in a CdTe module

the back metal of the CdTe TF cells. As T approaches the softening temperature of the EVA in the field or in a laboratory accelerated-exposure chamber, worm-like, cohesive-loss features (light gray) form as air is sucked into the module, forming the bubble that relieves the strain in the warped piece of glass. The finer structure at the lower left is a flaking of the back metal contact. PV response is almost always lost from these regions.

Glass strain and delamination can occur at the perimeter in the edge-deleted area due to 'pillowing'. Pillowing is caused by excessive squeezing at the edge due to the laminator pressure blatter. If, because of this, delamination occurs, it will happen between the glass/EVA interface. Further problems can ensue with water ingress and EVA swelling and softening.

If, on the other hand, the edge remains intact, pillowing can contribute to glass breakage before or after a module is in the field. Cracks will form just inside this perimeter where the bending stress is highest. These problems are caused by the neglect of proper edge shimming during lamination. The glass is bowed together and greatly stressed at the edge after it is removed from the laminator. Generally, shimming with slats that are slightly thicker than the finished laminate will eliminate this problem and provide a small compressive stress on the EVA at the perimeter. Delamination problems of this kind can be eliminated altogether, if one or both panels of glass are replaced with polymeric materials such as will be discussed in the next section.

Another kind of cracking that can propogate to the interior of tempered and untempered glass originates from stress points on the edge caused by improper handling before framing. 'Dings' caused by setting the edge of the glass module on a concrete floor, for example, provide points of stress for crack origination. Other kinds of module failure are accelerated when T is added to UV or moisture stresses. Browning of encapsulants[32] and polymer materials and loss of adhesion occur more rapidly at higher T.

Moisture

Moisture can reduce module reliability in a number of ways. The TF layers can be directly affected as in the example of CIGS already cited.[23] Module durability relies on the susceptibility of the TF cell materials to moisture *and* the ability of the module packaging to resist water ingress. Water/module interaction studies were performed at JPL in the 1980s and reported.[33] They point out that TF modules offer more direct surface and interfacial pathways for water to reach the cell materials than crystalline-Si type modules for two reasons: (1) the bulk Si cell is completely surrounded by encapsulant, whereas TF cell material is generally deposited on a substrate (usually conductive) and is not surrounded by encapsulant; (2) where TF cell materials are deposited on conductive glass superstrates, SnO_2 scribe lines, porous frit bridging conductors, and back metal isolation scribes offer ideal 'wicking' pathways for water to enter the structure. Mon *et al*.[33] report on the relative

importance of water ingress pathways and means to increase the module's resistance to the detrimental effects of water. It is generally expected that TF modules must pass 1000 h of chamber exposure to 85°C at 85% RH according to the IEEE 1262 or IEC 1215 qualification test procedures.

JPL evaluated the effectiveness of edge sealants on glass/glass coupons sealed with epoxies, butyls, and vinyl acetates.[33] Colbalt chloride humidity sensors were used to monitor the ingress of water during 300 h of stress at 85°C/100%RH. Only two of the epoxies survived the test. Today, more effective edge seal barrier schemes are being developed. In Free Energy Europe's fourth-generation framing, an 'appropriate adhesion treatment is (applied) on the glass, and advanced polymer material injected around the laminate'.[34] When sealing double-glass laminates of a-Si, they predict a 20-yr lifetime. Another company, Tru Seal[35] is offering a trial edge seal material, Insealedge[TM], which is being tested in prototype TF modules by several PV manufacturers. Additionally, they are offering an experimental lamination adhesive to replace EVA.

Adhesive bonds between the silane coupling agents dispersed in the encapsulant lamination material (e.g., EVA) and the glass or soft cover sheet must remain intact to prevent even more water ingress and delamination. When water reaches this interface, the siloxane bonds are hydrolysed.[36] De-adhesion can occur, which allows more rapid water ingress into the package. Extensive hydrothermal aging experiments[37] were conducted on EVA, EMA, PnBA, and polyurethane bonded to glass, metals and soft backsheet materials which included Tedlar, Scotchpar, Acrylar, Plexiglas, Korad 63000, Korad 212.

Wet resistance to de-adhesion can be promoted in different ways. When cross-linkable polymers are used to bond to glass as in PV, Coulter et al.[37] suggest addition of amines. A primer, designated as STR's A11861, composed of 9% benzyldimethylamine, 90% γ-MPS (methacryloxypropyltrimethoxysilane), and 1% Lupersol will increase wet resistance.[36] Peel strengths using A 11861 blended with the EVA showed increased adhesion to glass after 2 weeks water immersion and after 2 h boiling water.[37]

In addition, more chemically quantitative studies were carried out with primers on planar glass surfaces and on encapsulants loaded with glass beads.[38] Diffuse- and direct-transmittance Fourier transform infrared sampling techniques were used to evaluate the glass/primer interface. Samples were exposed to as much as 5000 h at 40°C, 2000 h at 60°C, and 1000 h at 80°C. Use of the glass bead sample configuration showed that the glass/EVA interface was extremely hygroscopic. Modulus, ultimate tensile strength, ultimate elongation, stretch and weight of absorbed water were measured during environmental testing. Silane coupling agents are found to delay hydrolysis at the bonding interface, but ultimately bonds are broken. Acid pretreatments can promote hydrothermal stability.[38] If interfacial bonds are broken, but silanol groups are not physically removed from the interface, bonds will be re-established. Individual water molecules are relatively harmless at the interface, unless they are capable of clustering into a liquid phase. Even if the interface remains intact, allowing for the reformation of bonds, the interphase region can be plasticized and weakened by water. Delamination can then occur by cohesive failure.[36] Surface and bulk conductivities are then increased, thereby compromising module safety due to electrical isolation problems as well as allowing the development of new failure mechanisms facilitated by these leakage currents (discussed later).

In the future, TF manufacturers would like to reduce the weight of double-glass-laminated modules by using soft polymeric backsheets and possibly frontsheets; some are already doing this. One successful example of a commercially available TF module packaged with soft front and backsheets is the United Solar Systems Corp. a-Si product. Crystalline Si modules have used Tefzel front covers or laminates of PET, Tedlar, and Al for the backsheets. To have TF modules survive damp heat, the water vapor transmission rates (WVTR) of these materials must be lowered. If Al is used to do this (backsheet only), it must be very thin so that no failures occur due to wrinkling during thermal cycling. Even then, a conductive backsheet can compromise safety.

Optically transparent gas-barrier thin films have been developed for food and medical packaging.[39] Companies are now developing silicon oxynitride carbide TF coatings for PET and Tefzel to enhance both the WVTR and adhesion properties.[40] Simple coatings at 25°C have WVTRs as low as 10^{-2} g m^{-2} d^{-1} and multilayers of organic/inorganic layers developed for the OLED industry[41] are below 10^{-5} g m^{-2} d^{-1}. WVTRs of these multilayers measure below 8×10^{-5} g m^{-2} d^{-1} at 85°C/50%RH. Additionally, the adhesion of untreated PET to EVA can be improved[42] from 1·5 N/mm to over 10 N/mm for coated PET. Resistance to UV and damp heat is reported.[42] The compressional stress in these films must be less than 5×10^9 dynes/cm^2 or they will develop microcracks during lamination.[42]

In order to account for moisture-related mechanisms quantitatively, the kinetics of moisture ingress and egress must be considered. Problems of moisture ingress into and through PV organic laminates under accelerated and field conditions need to be treated in the same way as these problems were treated in the electronic packaging industry.[43–46] Combinations of stresses are important. UV with elevated T can compromise adhesion and WVTR of encapsulant materials. In order to characterize these materials in a meaningful way, WVTR and adhesion have to be measured at field stress conditions, before and after weathering.

Attempts have been made to model the effect of water vapor on aging of PV materials. For normal and stressed operating conditions, the quantitative importance of moisture as a liquid and a vapor must be investigated. In cell-to-frame leakage current studies by G. Mon *et al.*[47] on small test modules encapsulated with PVB or EVA, an empirical approach is used that equates the relative effects of T and RH. They submit that 1%RH has about the same effect as 1°C. An old study on the relative effects of T and RH on polyvinyl butyral (PVB) by Cuddihy[48] found that each %RH has the same effect as each °C on the bulk electrical conductivity, and by inference the corrosion lifetime of encapsulated devices. He plotted the bulk conductivity of PVB supplied by J. Orehotsky at $T = 30°$, $40°$, and $50°C$ and RH = 54%, 80%, 85%, and 100% to determine this simple rule. Electrochemical corrosion due to currents through PVB could be expected to obey this summation of °C and RH. He went on to show that this simple relation does not exist between T and the partial pressure of water.

Generalizations of such a rule to failure mechanisms not controlled by the bulk conductivity of PVB must be developed. In fact, if EVA is the insulator, a review of the conductivity data[49] shows that 3.3% RH is equivalent to 1°C. The edge-deleted region of the modules is very vulnerable to the effects of water in terms of adhesion and voltage isolation.[50] Because the SnO_2 has been removed by mechanical abrasion, usually SiO_2 bead blasting, barrier coatings to prevent out-diffusion of Na are also removed.

Corrosion of soda-lime glass is another direct consequence of water; this can be a problem if small amounts of water come in contact with the glass surface.[51] Additionally, water that forms conducting paths where electrical isolation is required contributes to failure due to electrochemical corrosion or even arcing. Cell-to-frame currents are greatly increased due to high humidity or wet conditions on all module types.[49,52] These currents are particularly damaging on TF-superstrate modules where so-called 'bar-graph' patterning is observed (see below).

At an encapsulant/metal or encapsulant/glass interface good bonding is equivalent to good corrosion protection. The same silane interface chemistry used to promote bonding is used to prevent the corrosion processes on metal surfaces.[53] Metals such as Al that are commonly used as the last layer of a back contact on a solar cell are subject to corrosion in the presence of atmospheric and contaminant impurities.[54] Surface preparation and cleanliness before lamination cannot be over-stressed. A completely bonded laminant interface without contaminants eliminates the presence of corrosion cells and allows for a durable interface.[53]

A satisfactory solution to moisture-related defect mechanisms could be the development of a barrier coat directly deposited on the TF module materials and contacts. Such an attempt was made to coat superstrate a-Si module surfaces before encapsulation with an inorganic dielectric coating developed by Dow Corning.[55] Damp heat (85°C/85%RH) protection was successfully achieved for Al-coated glass contacts, but the sol–gel processing temperature of 400°C damaged the a-Si cells. When modules were coated at 250°C, micro-cracking was observed. Barrier coats of a sol–gel of this type or some of the barrier coats mentioned above may provide substantial protection of TF cells from water.

(High) voltage

Cell-to-frame leakage current, which may or may not involve water, has emerged as a problem for TF module manufacturers where SnO_2-coated soda-lime glass is used as a superstrate.[49,52,56,57] System voltages in utility applications are typically 600 V. Positive and negative potentials exist from the cells in the module to the module ground, which in most cases is the metal framing material. Figure 5 shows leakage-current pathways, and any one of these three currents can dominate, depending upon RH and T. Values for each I_i were calculated and compared with experiment.[56,57] Conductivity values for EVA, interfaces and surfaces were available elsewhere.[52] The bulk conductivity of the soda-lime glass is ionic, due to Na, and has an activation energy[58] of 0·8 eV.
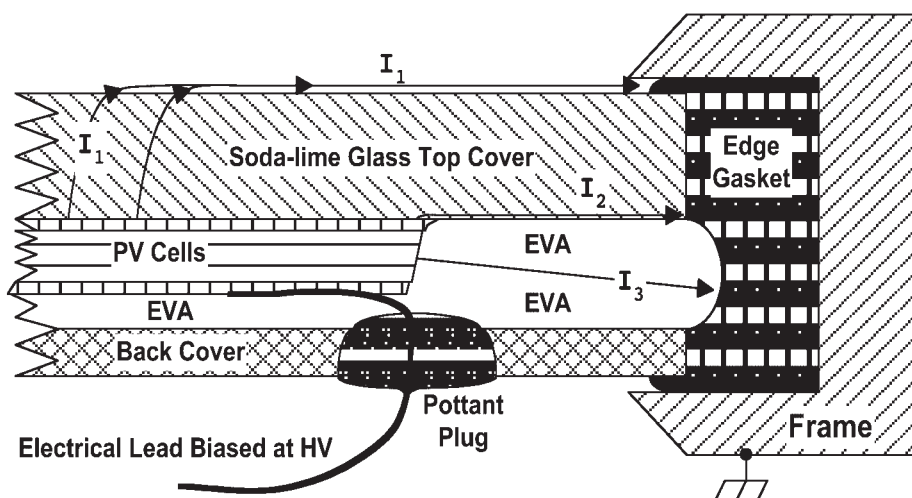
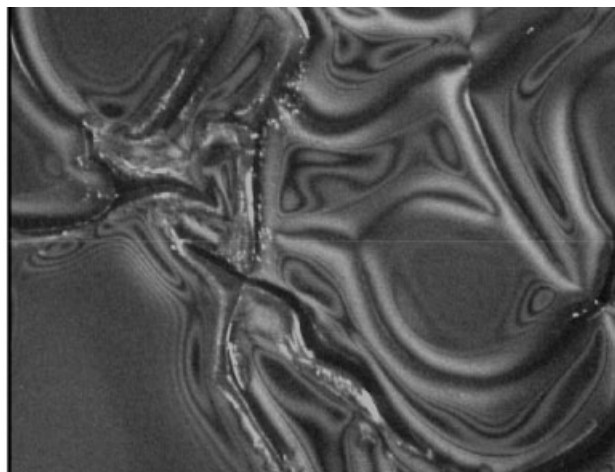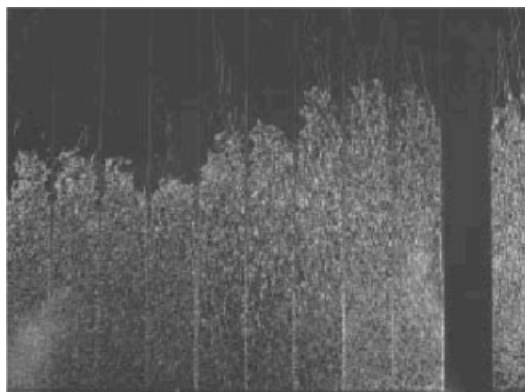Figure 5. Cross-section of edge-seal region of a thin-film module[56]

Figure 6. 'Bar-graph' delamination of a-Si cells, left[55]; 100x closeup showing interference fringes due to delamination of the SnO_2 from the glass interface, right

When the glass is warm to hot, and it is humid or the front surface has condensed water, I_1 dominates. With the cells biased negative relative to ground, the most destructive condition for the SnO_2/glass interface exists. Figure 6 is one picture of such damage.[57] Na ions drift to the interface where they corrode/decompose the glass at the interface or react with water and form H that reduces the SnO_2; each process is capable of reducing adhesion at that interface. The SnO_2 and/or the SiO_2 barrier layer delaminates from the glass:[57,59] This layer and the cells deposited on it crack and curl into the EVA, resulting in the bar-graph-damage patterning in Figure 6. Using damage area as the parameter with which to measure the progression of damage, an activation of 0·78 eV was found, which agrees with a damage mechanism involving Na drift.[57,58]

At lower *T* and/or dryer conditions, I_2 and I_3 dominate. These currents have been calculated based on relative humidity exposure values for bulk conductivities of EVA and interface conductivities with soda-lime glass.[52] As this interface has been shown to be extremely hydrophillic,[37] these leakage currents can be much worse than calculations suggest. Module safety and durability become irreversibly compromised.

Other high-voltage safety problems can develop if conductive backsheets are used. Generally, these are Al foils laminated to a polymer film or a polymer such as PET coated with Al to a thickness that will serve as an

effective moisture barrier. A metal frame in such close proximity to a conductive sheet that is less than 1 mm from the module's back metal contact over the entire area of the module can become problematic (see next section).

Thermal cycling, humidity–freeze and current

Thermal cycling and humidity–freeze are severe tests of the mechanical strength and design of the module package. Water may indirectly contribute to the failure that will be discussed in this section. Full-size modules are usually required because stress/strain due to differences in thermal expansion will increase with size. The IEEE 1262 PV module qualification test includes 10 cycles of humidity–freeze that hold the module for 20 h at 85°C/85% RH, followed by 1 h at −40°C. These tests also include up to 200 cycles of thermal cycling between 85°C and −40°C.

Thermal cycling can cause wrinkling of a soft backsheet, especially if an Al foil is included with a thickness great enough for its mechanical strength to move the backsheet across the soft EVA during the high-T portion of the cycle. The shear stress that develops during each cycle is released as the backsheet slowly wrinkles. This can produce high-voltage arcing points at the module frame or in the junction box.

Another thermal coefficient of expansion-mismatch-induced failure can occur outdoors in TF modules. At NREL, we have observed failure of the solder bonding of the Cu ribbon to the Ag frit on occasion, presumably due to the bonding fatigue. This may not have occurred during the original IEEE 1262 testing because module bias currents of the order of the short-circuit current were never applied during temperature cycling. Outdoor stress has diurnal heating cycles that fatigue solder bonds and mechanically susceptible points in conductors. This degradation is enhanced by localized heating at the solder bond caused by the module's current output. A revised IEEE test sequence will include current bias during temperature cycling.

When moisture is present, small currents can cause electrochemical and galvanic corrosion[60] and electrolytic metallic electromigration.[61] Mon et al.[60] report on results from studies at JPL on a-Si modules with Al-contacts. Electrolytic corrosion is driven by the applied or photovoltaically generated potential difference between contacts separated by an ionically conductive median. Oxidation of the anode and plating at the cathode result in the dissolution of the back contact metal and shorting between the cell elements. The authors report on corrosion processes of this type occurring at room temperature for a number of different electrode materials including SnO_2-coated glass. Small corrosion potentials of 0·5 V result in a low inter-electrode current of 1·5 mA that, with humidity exposure, produces a bar-graph patterning.

Galvanic corrosion occurs when two dissimilar material conductors are separated by an electrolytic median; no applied electric potential is necessary. TF superstrate modules incorporate a conductive SnO_2 film coated on the inside of the front glass. Many manfacturers include a Ag frit. Back-contact metals are Al, Ni, and/or Ag, with other metals added to levels of several percent. JPL tested galvanic corrosion effects on encapsulated and un-encapsulated metal-coated glass samples exposed to damp heat. Results vary depending on metal used and type of glass (soda-lime or borosilicate).[60]

Electromigration, a solid-state process that usually requires high current densities and elevated temperature has been noted to occur at the Al scribe-line interconnects of a-Si modules.[61] Krumbein et al.[62] detail electrolytic electromigration, as distinguished from the solid state electromigration. 'Wet' and 'humid' processes are discussed, as well as the role of contaminants. Each type of corrosion mechanism has is own unique visual signature. Proper interpretation of damage, much of which can be done visually, is critical to identify relevant failure mechanisms.

CONCLUSIONS

A table is developed that shows TF PV cell and module failure modes and suspected mechanisms. Module- and packaging-related problems specific to TF modules are reviewed. These are categorized according to the type of stress that produced them, e.g., temperature, voltage, moisture, current, and thermal cycling. A graph is developed to relate time under indoor accelerated stress to time at three outdoor use sites for thermally activated

processes. Diagnostic tools for locating the affected area within these large-area modules are reviewed. Identification of damage mechanisms by visual appearance is stressed. The edge-deleted perimeter of SnO_2-coated glass modules is an area of continued concern for reliable module encapsulation.

Acknowledgements

REFERENCES

1. *Photovoltaics Energy for the New Millennium: The National Photovoltaics Program Plan*, DOE/GO-10099-940, January 2000; 15.
2. McMahon TJ, Jorgensen GJ, Hulstrom RL, King DL, Quintana MA. Module 30-year life—What does it mean? and is it predictable/achievable? *NCPV Program Review Meeting*, Denver, 16–19 April 2000.
3. Ross RG. Crystalline-silicon reliability lessons for thin-film modules. *Proceedings of the 18th IEEE PV Specialists Conference*, Las Vegas, 1985; 1014.
4. Quintana MA, King DL, McMahon TJ, Osterwald CR. Commonly observed degradation in field-aged PV modules. *Proceedings of the 29th IEEE PV Specialists Conference*, New Orleans, 2002; 1436.
5. Meeker WQ, Hahn GJ. How to plan an accelerated life test—some practical guidelines. In *The ASQC Basic References in Quality Control: Stastical Techniques*, Cornell JA, Shapiro SS (eds). ASQC Quality Press: Milwaukee, 1985.
6. AMPS-1D. A one-deminsional device simulation program for the analysis of microelectronic and photonic structures. Written under the direction of S. Fonash, Pennsylvania State University, and supported by EPRI.
7. McMahon TJ, Fahrenbruch AL. Insights into the non-ideal behavior of CdS/CdTe solar cells. *Proceedings of the 28th IEEE PV Specialists Conference*, Anchorage, 2000; 539.
8. King DL, Kratochvil JA, Quintana MA, McMahon TJ. Applications for infrared imaging equipment in photovoltaic cell, module, and system testing. *Proceedings of the 28th IEEE PV Specialists Conference*, Anchorage, 2000; 1436.
9. McMahon TJ, Rummel SR, Basso TS. Cell shunt resistance on PV module performance. *Proceedings of the 25th IEEE PV Specialists Conference*, Washington, DC, 1996; 1291.
10. Abete A, Cane F, Rizzitano C, Tarantino M, Tomnasini R. Performance testing procedures for photovoltaic modules in mismatching conditions. *Proceedings of the IEEE PV Specialists Conference*, Las Vegas, NV, 1991; 807.
11. Maire J, Theys B, Baruch P. Detection of a defective cell in a solar module through photoresponse modulation. *Proceedings of the IEEE PV Specialists Conference*, Kissimmee, FL, 1981; 1134.
12. Baruch P, Benghanem B, Leroy B, Picard C, Roger JA. Analysis of photovoltaic generators by modulated light excitation of individual cells: application to testing and detection of faulty cells. *Proceedings of the IEEE PV Specialists Conference*, Kissimmee, FL, 1984; 621.
13. Eisgruber IL, Sites JR. Extraction of individual-cell photocurrents and shunt resistances in encapsulated modules using large-scale laser scanning. *Progress in Photovoltaics: Research and Applications* 1996; **4**: 63.
14. Meeker WQ, Escobar LA. Pitfalls of accelerated testing. *IEEE Transactions on Reliability* 1998; **47**: 114.
15. McMahon TJ, Jorgensen GJ. Progress toward a CdTe Cell life prediction. *Proceedings of the 13th NREL Photovoltaic Program Review*, AIP Conference Proceedings 462, Denver, September 1998; 54.
16. Osterwald CR, Anderberg A, Rummel S, Ottoson L. Degradation analysis of weathered crystalline-silicon PV modules. *Proceedings of the 29th IEEE PV Specialists Conference*, New Orleans, 2002; 1392.
17. Frick NH. Experiences at quantifying degradation and assessing life potential of paints and coatings. *Proceedings of the Flat-Plate Solar Array Project Research Forum on Quantifying Degradation, JPL Publication* 83–52; 1983; 29.
18. Jorgensen G, Bingham C, King D, Lewandowski A, Netter J, Terwilliger K, Adamsons K. Use of uniformly distributed concentrated sunlight for highly accelerated testing of coatings. *ACS Symposium* Series 2002; **805**: 100–118.
19. UL 1703–1993. *Standard for Flat-Plate Photovoltaic Modules and Panels*. Northbrook, IL.
20. IEEE Recommended Practice for Qualification of Photovoltaic (PV) Modules. IEEE Standard 1262–1995, *IEEE*, 1996.
21. IEC 1215. Crystalline silicon terrestrial photovoltaic modules—design qualification and type approval. Bureau Central de la Commission Electrotechnique International, Geneva, 1993.

22. Block V solar cell module design and test specification for intermediate load conditions. JPL/5101-161, Jet Propulsion Laboratory, Pasadena, CA, 1981.

23. Wennerberg J, Kessler J, Stolt L. Degradation mechanisms of Cu(In,Ga)Se$_2$-based thin film PV modules. *Proceedings of the 16th European PV Solar Energy Conference*, 2000; 309 and Cu(In,Ga)Se$_2$-based thin-film photovoltaic modules optimized for long-term performance. *Solar Energy Materials and Solar Cells* 2003; **75**: 47.

24. Hegedus SS, McCandless BE, Birkmire RW. Analysis of stress-induced degradation in CdS/CdTe solar cells. *Proceedings of the 28th IEEE PV Specialists Conference*, Anchorage, 2000; 535.

25. Stollwerck G, Sites JR. *Proceedings of the 13th European Photovoltaic Solar Energy Conference*, Nice, France, October 1995; 2020 and McCandless BE, Phillips JE, Titus J. *Proceedings of the 2nd World Conference and Exhibition on PV Solar Energy Conversion*, 1998; 448.

26. Lathrop JW, Anderson PA. Failure mechanisms in a-Si Solar Cells. *Proceedings of the 19th IEEE PV Specialists Conference*, New Orleans, 1987; 200.

27. McMahon TJ, Bennett MS. Metastable shunt paths in a-Si solar cells. *Solar Energy Materials and Solar Cells* 1996; **41/42**: 465.

28. McMahon TJ. Dark current transients in thin-film CdTe solar cells. *Proceedings of the 29th IEEE PV Specialists Conference*, New Orleans, 2002; 768.

29. Shahidul Haque M, Naseem HA, Brown WD. Interaction of aluminum with hydrogenated amorphous silicon at low temperatures. *Journal of Applied Physics* 1994; **75**(8): 3928.

30. See text books, e.g., Mann NR, Schafer RE, Singpurwalla ND. *Methods for Statistical Analysis of Reliability and Life Data*. Wiley: New York; 1974.

31. Lindner A, Coussot P, Bonn D. Viscous fingering in a yield stress fluids. *Physical Review Letters* 2000; **85**: 314.

32. Pern FJ, Glick SH. Photothermal stability of encapsulated Si solar cells and encapsulation materials upon eccelerated exposure. *Solar Energy Materials and Solar Cells* 2000; **61**: 153.

33. Mon GR, Wen L, Ross R. Water-module interaction studies. *Proceedings of the 20th IEEE PV Specialists Conference*, Las Vegas, 1988; 1098.

34. van der Vleute F, Guillardeau D. Amorphous solar panels now affordable and reliable. www.FreeEnergyEurope.com

35. True Seal Technologies, 105 Grattan Road, Richmond, VA 23229, USA.

36. Pleuddemann EP. *Silane Coupling Agents*, Chap. 5, Plenum, New York, 1991.

37. Coulter DR, Cuddihy EF, Plueddemann EF. Chemical bonding technology for terrestrial photovoltaic modules. *JPL Document 5101-232*, DOE/JPL 1012-91, Jet Propulsion Laboratory, Pasadena, 1983.

38. Koenig JL, Boerio FJ, Plueddemann EF, Miller J, Willis PB, Cuddihy EF. Chemical bonding technology: direct investigation of interfacial bonds. *JPL Document 5101-284*, DOE/JPL 1012-120, Jet Propulsion Laboratory, Pasadena, 1986.

39. Brody AL. Glass-coated flexible films for packaging: an overview. *Packaging Technological Engineering*, February 1994, 44.

40. AKT, 3101 Scott Blvd, Santa Clara, CA; Isovolta, A-2355 Wr. Neudorf, Austria.

41. Burrows PE, Graff GL, Gross ME, Martin PM, Hall M, Mast E, Bonham C, Bennett W, Michalski L, Weaver M, Brown JJ, Fogarty D, Sapochak LS. Gas permeation and lifetime tests on polymeric-based barrier coatings. *Proceedings of the SPIE Annual Meeting*, San Diego, CA, 30 September 2000; 75–83.

42. Barber G, Jorgensen G, Terwilliger K, Pern J, Glick S, McMahon TJ. New barrier coating materials for PV module backsheets. *Proceedings of the 29th IEEE PV Specialists Conference*, New Orleans, 2002; 1541.

43. Pecht MG, Ardebili H, Shukla AA, Hagge JK, Jennings D. Moisture ingress into organic laminates. *IEEE Transactions on Components and Packaging Technology* 1999; **22**: 104.

44. Ardebili H, Hillman C, Natishan MAE, McCluskey P, Pecht MG, Peterson D. A comparison of the theory of moisture diffusion in plastic encapsulated microelectronics with moisture chip and weight-gain measurements. *IEEE Transactions on Components and Packaging Technology*, 2002; **25**: 132.

45. Tencer M. Moisture ingress into non-hermetic enclosures and packages: a quasi-steady state model for diffusion and attenuation of ambient humidity variations. *Proceedings of the 44th IEEE Electronic Components and Technology Conference*, Washington, DC, 1–4 May 1994; 196–209.

46. Schnable GL, Comizzoli RB, Kern W, White LK. A survey of corrosion failure mechanisms in microelectronic devices. *RCA Review* 1969; **40**: 416.

47. Mon GR, Wen L, Ross RG, Adent D. Effects of temperature and moisture on module leakage currents. *Proceedings of the 18th IEEE PV Specialists Conference*, Las Vegas, 1985; 1179.

48. Cuddihy EF. The aging correlation (rh + T): relative humidity (%) + temperature (°C). *JPL Document 5101–283*, DOE/JPL 1012–121, Jet Propulsion Laboratory, Pasadena, 1986.

49. Mon GR, Ross R. Electrochemical degradation of amorphous silicon photovoltaic modules. *Proceedings of the 18th IEEE PV Specialists Conference*, Las Vegas, 1985; 1142.
50. McMahon TJ, Jorgensen GJ. Electrical currents and adhesion of edge-deleted regions of EVA-to-glass module packaging. *Proceedings of the 2001 NCPV Program Review Meeting*, Lakewood, CO, October 2001; 137–138.
51. Charles RJ. Static fatigue of glass. *Journal of Applied Physics* 1958; **29**: 1549.
52. Mon GR, Wen L, Ross RG. Encapsulant-free surfaces and interfaces: critical parameters in controlling cell corrosion. *Proceedings of the 19th IEEE PV Specialists Conference*, New Orleans, 1987; 1215.
53. Tonge J. DOW Chemical Corporation.
54. Graedel TE. Corrosion mechanisms for aluminun exposed to the atmosphere. *Journal of the Electrochemical Society* 1989; **136**: 204C.
55. Longrigg P. An investigation into the use of inorganic coatings for thin-film photovoltaic modules. *Solar Cells* 1989; **27**: 267.
56. del Cueto JA, McMahon TJ. Analysis of leakage currents in photovoltaic modules under high-voltage bias in the field. *Progress in Photovoltaics Research and Applications* 2002; **10**: 15.
57. Osterwald CR, McMahon TJ, del Cueto JA. Electrochemical corrosion of SnO_2:F transparent conducting layers in thin-film PV modules. *Solar Energy Materials and Solar Cells* 2003; **79**: 21–33.
58. Tooley FV. *The Handbook of Glass Manufacture*, Vol. II, 3rd edn. Ashlee: New York, 1984; 944.
59. Carlson DE, Romero R, Willing F, Meakin D, Gonzalez L, Murphy R, Moutinho HR, Al-Jassim M. Corrosion effects in thin-film photovoltaic modules. *Progress in Photovoltaics* 2003; **11**: 377–386.
60. Mon GR, Wen L, Meyer J, Nelson A, Ross R. Electrochemical and galvanic corrosion effects in thin-film photovoltaic modules. *Proceedings of the 20th IEEE PV Specialists Conference*, Las Vegas, 1988; 108.
61. Wen L, Mon G, Jetter R, Ross R. Electromigration in thin-film photovoltaic module metalization systems. *Proceedings of the 20th IEEE PV Specialists Conference*, Las Vegas, 1988; 364.
62. Krumbein SJ. Tutorial: electrolytic models for metalic electromigration failure mechanisms. *IEEE Transactions on Reliability* 1995; **44**: 539.